Electronic Supplementary Material (ESI) for Physical Chemistry Chemical Physics.

Supporting Information

^{13}C-^{13}C Spin-Coupling Constants in Crystalline ^{13}C-Labeled Saccharides: Conformational Effects Interrogated by Solid-State ^{13}C NMR Spectroscopy

Wenhui Zhang,[1] Mi-Kyung Yoon,[1] Reagan J. Meredith,[1] Matthew Hadad,[1] Jaroslav Zajicek,[1] Michael H. Frey,[3] Allen G. Oliver,[1] Ian Carmichael,[2] and Anthony S. Serianni[1]*

[1]Department of Chemistry and Biochemistry, and [2]Radiation Laboratory, University of Notre Dame, Notre Dame, IN 46556-5670; [3]JEOL USA, Inc., 11 Dearborn Rd., Peabody, MA 01960 USA

Table of Contents

1. Chemical synthesis procedures to prepare ^{13}C-labeled **3** S2
2. Chemical synthesis procedures to prepare **2**$^{1',5}$ and **4**$^{1',5}$ (Scheme S1) S3
3. Table S1. HRMS (ESI-TOF) data for ^{13}C-labeled **2**–**4** S6
4. Figure S1. Partial $^{13}C\{^1H\}$ NMR spectrum (150 MHz) of **3**^{1,2} S7
5. Figure S2. Partial $^{13}C\{^1H\}$ NMR spectrum (150 MHz) of **3**^{1,3} S8
6. Figure S3. Partial $^{13}C\{^1H\}$ NMR spectrum (150 MHz) of **3**^{1,6} S9
7. Figure S4. Partial $^{13}C\{^1H\}$ NMR spectrum (150 MHz) of **2**$^{1',5}$ S10
8. Figure S5. Partial $^{13}C\{^1H\}$ NMR spectrum (150 MHz) of **4**$^{1',5}$ S11
9. Scheme S2. Torsional constraints applied to **2**^{c} and **4**^{c} during DFT calculations S12
10. Table S2. ^1H-^1H spin-couplings in **2**–**4** S13
11. Table S3. Fitting statistics from solid-state ^{13}C NMR determinations of J_{CC} values in crystalline **2**$^{1',5}$, **3**^{1,2}, **3**^{1,3}, **3**^{1,6} and **4**$^{1',5}$ S14
12. Figure S6. Plots of $^3J_{C1',C5}$ versus ψ for **2**^{k} and **4**^{k} S15
13. Figure S7. Plots of $^3J_{C1',C5}$ in **2**^{k} and **4**^{k} as a function of ψ S16
14. Cartesian coordinates for DFT structures **2**^{k}–**4**^{k} S17
15. Complete reference 40 S20

1. *Chemical Synthesis of ^{13}C-Labeled **3***

^{13}C-Labeled D-glucose (**5**^{1,2}, **5**^{1,3} or **5**^{1,6}) (500 mg, 2.75 mmol) was dissolved in anhydrous methanol (50 mL), a heterogeneous acid catalyst (dry Dowex 50 x 8 (50–100 mesh) cation-exchange resin in the H^+ form; 1.0 g) was added, and the reaction mixture was refluxed for 20 h.[1] After cooling and filtration to remove the resin, the filtrate was concentrated to a stiff syrup at 30 °C *in vacuo* and the syrup was dissolved in distilled/deionized (DI) water (1.0 mL). The aqueous solution was applied to a 2.5 cm x 50 cm chromatographic column containing Dowex 1 x 8 (200–400 mesh) ion-exchange resin in the OH^- form.[2] The column was eluted with DI water, and fractions (15 mL) were collected and analyzed by ^{1}H NMR. ^{13}C-Labeled methyl α-D-glucopyranoside (**6**) eluted in fractions 24–28. Fractions 35–39 containing ^{13}C-labeled methyl β-D-glucopyranoside (**3**) were pooled, concentrated at 30 °C *in vacuo*, and pure ^{13}C-labeled **3** was crystallized from a concentrated aqueous solution.

References

1. C. A. Podlasek, J. Wu, W. A.Stripe, P. B. Bondo and A. S. Serianni, [^{13}C]Enriched Methyl Aldopyranosides: Structural Interpretations of ^{13}C-^{1}H Spin-Coupling Constants and ^{1}H Chemical Shifts. *J. Am. Chem. Soc.* 1995, **117**, 8635–8644.
2. P. W. Austin, F. E. Hardy, J. C. Buchanan and J. Baddiley, The Separation of Isomeric Glycosides on Basic Ion-Exchange Resins, *J. Chem. Soc*. 1963, 5350–5353.

2. *Chemical Synthesis of Disaccharides* ***2***$^{1',5}$ *and* ***4***$^{1',5}$ (Scheme S1)

A. 2,3,4,6-Tetra-O-acetyl-α-D-[1-^{13}*C]galactopyranosyl trichloroacetimidate (**8**).* D-[1-^{13}C]Galactose (**7**) (1.00 g, 5.52 mmol) was dissolved in pyridine (20 mL) and acetic anhydride (3.10 mL, 33.1 mmol) was added. The reaction mixture was stirred at rt overnight and concentrated at 30 °C *in vacuo* to afford D-[1-^{13}C]galactopyranose pentaacetate. The pentaacetate was selectively deacetylated at C1 with benzylamine (0.75 mL, 6.90 mmol) in THF (30 mL). After purification on a silica gel column, the tetraacetate product (1.54 g, 4.42 mmol) was converted to the corresponding trichloroacetimidate with trichloroacetonitrile (1.77 mL, 17.68 mnol) and 1,8-diazobicyclo [5.4.0]-undec-7-ene (DBU, 60 μL) in DCM (30 mL), affording **8** as a white foam (1.66 g, 3.37 mmol, 61%).

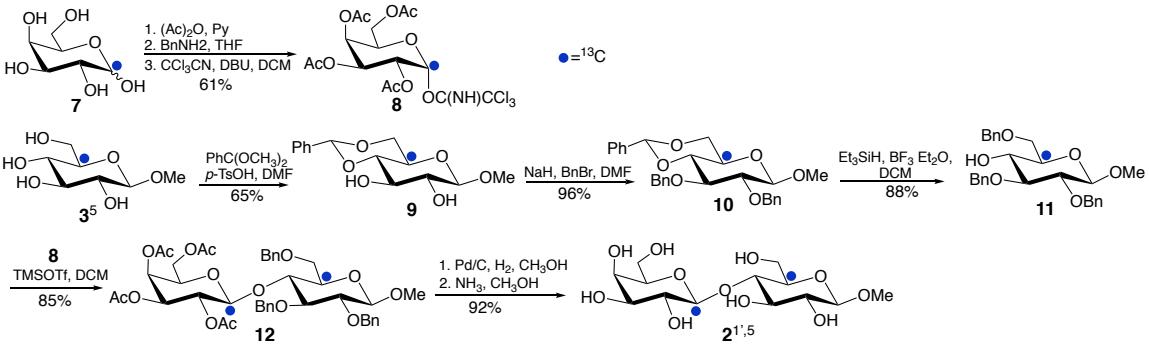

Scheme S1

B. Methyl 4,6-O-benzylidene-β-D-[5-^{13}*C]glucopyranoside (**9**).* Methyl β-D-[5-^{13}C]glucopyranoside (**3**^{5}) was prepared from D-[5-^{13}C]glucose (**5**^{5}) using the same procedure to prepare ^{13}C-labeled **3**^{1,2} (see above). Compound **3**^{5} (0.97 g, 5.00 mmol) was dissolved in dry *N,N*-dimethylformamide (DMF) (30 mL), and benzaldehyde dimethylacetal (0.91 mL, 6.25 mmol) and a catalytic amount of *p*-toluenesulfonic acid were added. The reaction mixture was stirred at 50 °C for 22 h and neutralized by adding one drop of triethylamine. The DMF was removed at 30 °C *in vacuo* on a rotovap, the syrup was dissolved in CH_2Cl_2, and the resulting solution washed with water. The organic phase was dried over Na_2SO_4 and then concentrated at 30 °C *in vacuo* to a syrup. Methyl

glycoside **9** was isolated by crystallization from hexanes/ethyl acetate (0.92 g, 3.25 mmol, 65%).

*C. Methyl 2,3-di-O-benzyl-4,6-O-benzylidene-β-D-[5-^{13}C]glucopyranoside (**10**)*. Compound **9** (0.90 g, 3.24 mmol) was dissolved in DMF (30 mL) and NaH (60%, 0.52 g, 13.0 mmol) was added to the solution. After stirring at rt for 30 min, benzyl bromide (1.60 mL, 13.0 mmol) was added dropwise at 0 °C and the mixture was stirred at rt overnight. The mixture was then diluted with CH_2Cl_2 (50 mL) and washed with water. The organic phase was dried over anhydrous Na_2SO_4, concentrated at 30 °C *in vacuo* to dryness, and the residue purified by flash chromatography on a silica gel column (2.5 cm x 30 cm) (solvent: hexanes/ethyl acetate 4:1) to afford **10** as a white solid (1.44 g, 3.11 mmol, 96%).

*D. Methyl 2,3,6-tri-O-benzyl-β-D-[5-^{13}C]glucopyranoside (**11**)*. Compound **10** (1.40 g, 3.02 mmol) was dissolved in anhydrous CH_2Cl_2 (40 mL), and triethylsilane (4.85 mL, 30.2 mmol) and $BF_3{\cdot}Et_2O$ (0.75 mL, 6.04 mmol) were added at 0 °C. The reaction mixture was stirred at rt for 5 h. The mixture was diluted with CH_2Cl_2 (40 mL) and the resulting solution was washed with aqueous $NaHCO_3$ solution (1 *M*) (20 mL), followed by distilled water (40 mL). The organic phase was dried over Na_2SO_4 and concentrated at 30 °C *in vacuo* to dryness. The residue was purified by flash chromatography on a silica gel column (2.5 cm x 40 cm) (solvent: hexanes/ethyl acetate, 3:1) to afford **11** as a colorless syrup (1.23 g, 2.65 mmol, 88%).

*E. Methyl 2,3,4,6-tetra-O-acetyl-β-D-[1-^{13}C]galactopyranosyl-(1→4)-2,3,6-tri-O-benzyl-β-D-[5-^{13}C]glucopyranoside (**12**)*. Donor **8** (1.61 g, 3.27 mmol) and acceptor **11** (1.20 g, 2.60 mmol) were dissolved in anhydrous CH_2Cl_2 (50 mL) after drying over high vacuum, and the solution was treated with molecular sieves (4 Å, 4.0 g). A catalytic amount of trimethylsilyltriflate (50 μL, 0.26 mmol) was added at 0 °C. The reaction mixture was stirred at rt for 2 h, neutralized with the addition of triethylamine (50 μL), and filtered to remove the molecular sieves. The filtrate was concentrated at 30 °C *in vacuo* and the resulting syrup was purified by flash chromatography on a silica gel column (2.5 cm x 40

cm) (solvent: hexanes/ethyl acetate, 2:1) to afford **12** as a white foam (1.74 g, 2.20 mmol, 85%).

*F. Methyl β-D-[1-^{13}C]galactopyranosyl-(1→4)-β-D-[5-^{13}C]glucopyranoside (**2**$^{1',5}$).* Disaccharide **12** (1.74 g, 2.20 mmol) was dissolved in methanol (50 mL) and treated with Pd/C (10%, 400 mg) and H_2 overnight. The Pd/C was removed by filtration and the filtrate was saturated with NH_3 (*g*). After 20 h, the reaction mixture was concentrated at 30 °C *in vacuo.* The residue was dissolved in ~1 mL of distilled water and the solution was applied to a column (2.5 x 100 cm) containing Bio-Gel P-2 resin. The column was eluted with DI water at ~1.0 mL/min, and fractions (~15 mL) were collected and assayed by ^{1}H NMR. Fractions (25–29) containing the product were pooled and concentrated at 30 °C *in vacuo* to give disaccharide **2**$^{1',5}$ (0.72 g, 2.02 mmol, 92%). Disaccharide **2**$^{1',5}$ was crystallized from methanol for use in X-ray structure analysis and NMR *J*-coupling measurements.

*G. Methyl β-D-[1-^{13}C]galactopyranosyl-(1→4)-α-D-[5-^{13}C]glucopyranoside (**4**$^{1',5}$).* Starting with methyl α-D-[5-^{13}C]glucopyranoside (**6**^{5}), methyl β-D-[1-^{13}C]galactopyranosyl-(1→4)-α-D-[5-^{13}C]glucopyranoside (**4**$^{1',5}$) was prepared by the same procedure used to prepare compound **2**$^{1',5}$ and was crystallized from methanol.

Table S1. HRMS (ESI-TOF) Data[a] for ^{13}C-Labeled **2**–**4**.

***m/z* value**	**compound**				
	2$^{1',5}$	**3**^{1,2}	**3**^{1,3}	**3**^{1,6}	**4**$^{1',5}$
calculated *m/z* $[M + Na]^+$	381.1216	219.0688	219.0688	219.0688	381.1216
found *m/z* $[M + Na]^+$	381.1229	219.0748	219.0761	219.0735	381.1209

[a]Data were obtained on a BRUKER micrOTOF-Q II instrument with an ESI source. The dry heater was set at 180 °C and the nebulizer was set at 0.4 Bar. The capillary voltage was 4.5 kV and the end plate offset was –0.5 kV. Full MS scans were collected over a range of 50–1650 *m*/*z*.

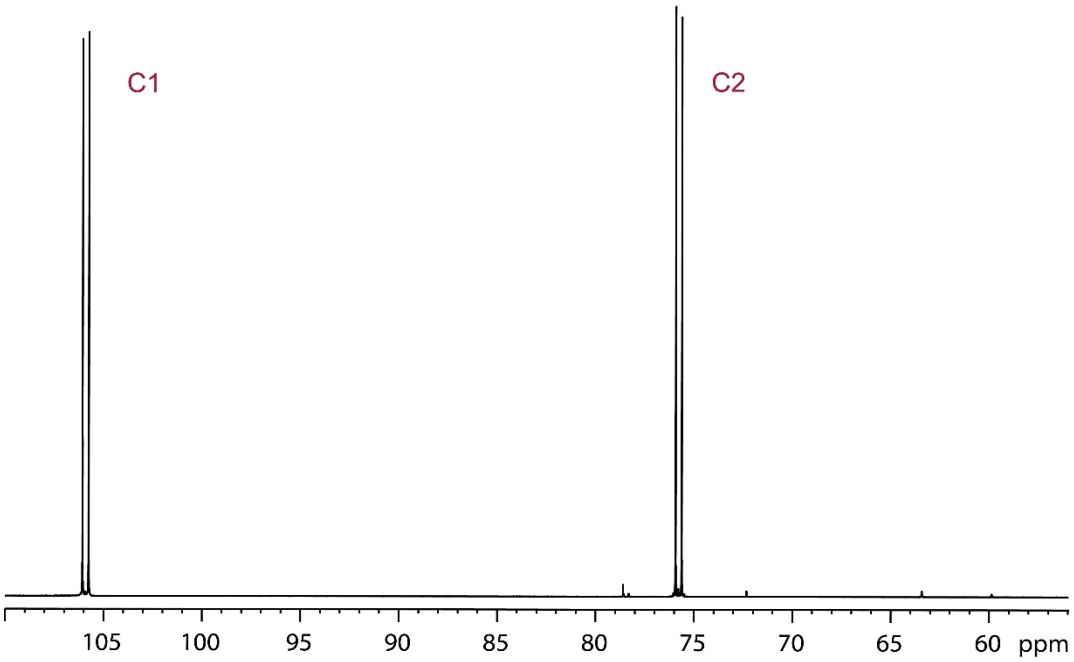

Figure S1. Partial $^{13}C\{^{1}H\}$ NMR spectrum (150 MHz) of methyl β-D-[1,2-$^{13}C_2$]glucopyranoside (**3**$^{1,2)}$. Signal assignments are shown for the ^{13}C-labeled carbons and the weak signals (60–80 ppm) arise from carbons at natural abundance. $^{1}J_{C1,C2}$ (46.8 Hz) was measured from the splittings of the C1 and C2 signals.

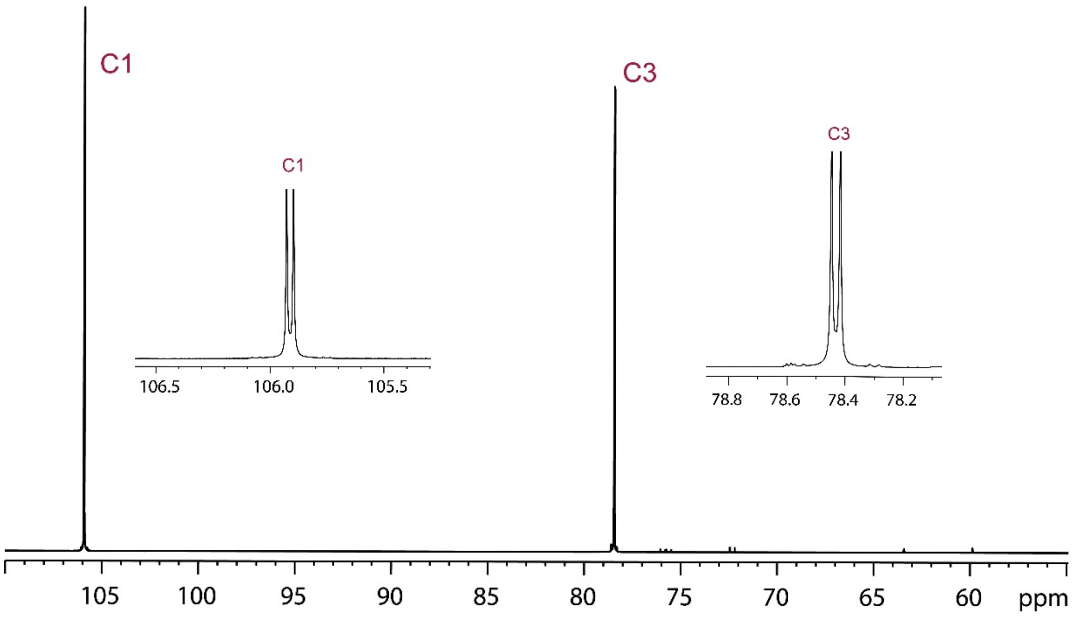

Figure S2. Partial $^{13}C\{^{1}H\}$ NMR spectrum (150 MHz) of methyl β-D-[1,3-$^{13}C_2$]glucopyranoside (**3**^{1,3}). Signal assignments shown are shown for the ^{13}C-labeled carbons and the weak signals (60–80 ppm) arise from carbons at natural abundance. $^{2}J_{C1,C3}$ (+4.6 Hz) was measured from the splittings (insets) of the C1 and C3 signals.

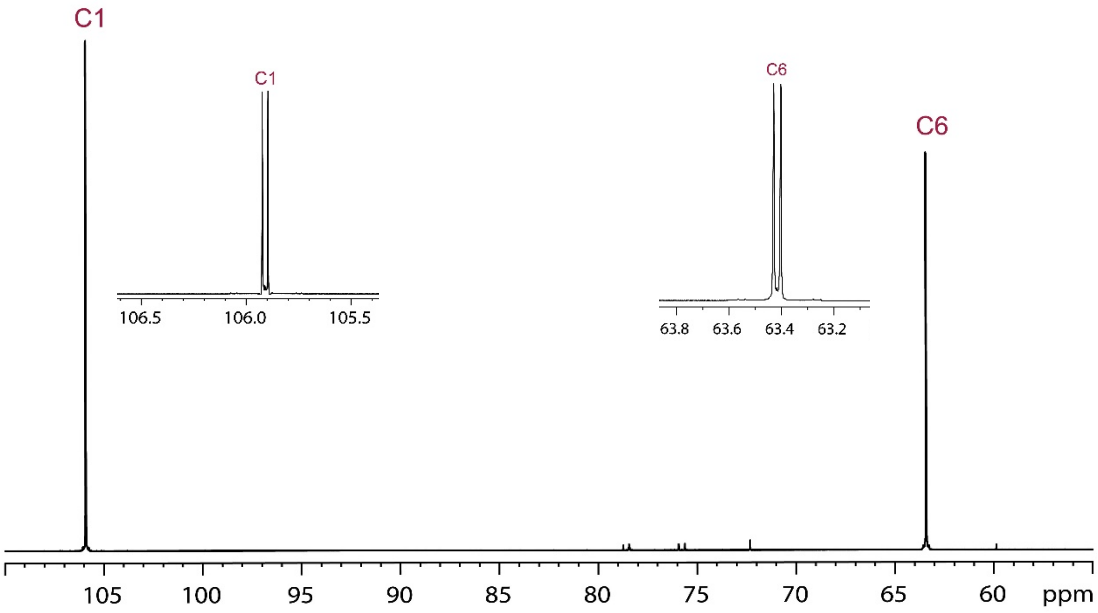

Figure S3. Partial $^{13}C\{^{1}H\}$ NMR spectrum (150 MHz) of methyl β-D-[1,6-$^{13}C_2$]glucopyranoside (**3**^{1,6}). Signal assignments are shown for the ^{13}C-labeled carbons and the weak signals (60–80 ppm) arise from carbons at natural abundance. $^{3}J_{C1,C6}$ (4.1 Hz) was measured from the splittings (insets) of the C1 and C6 signals.

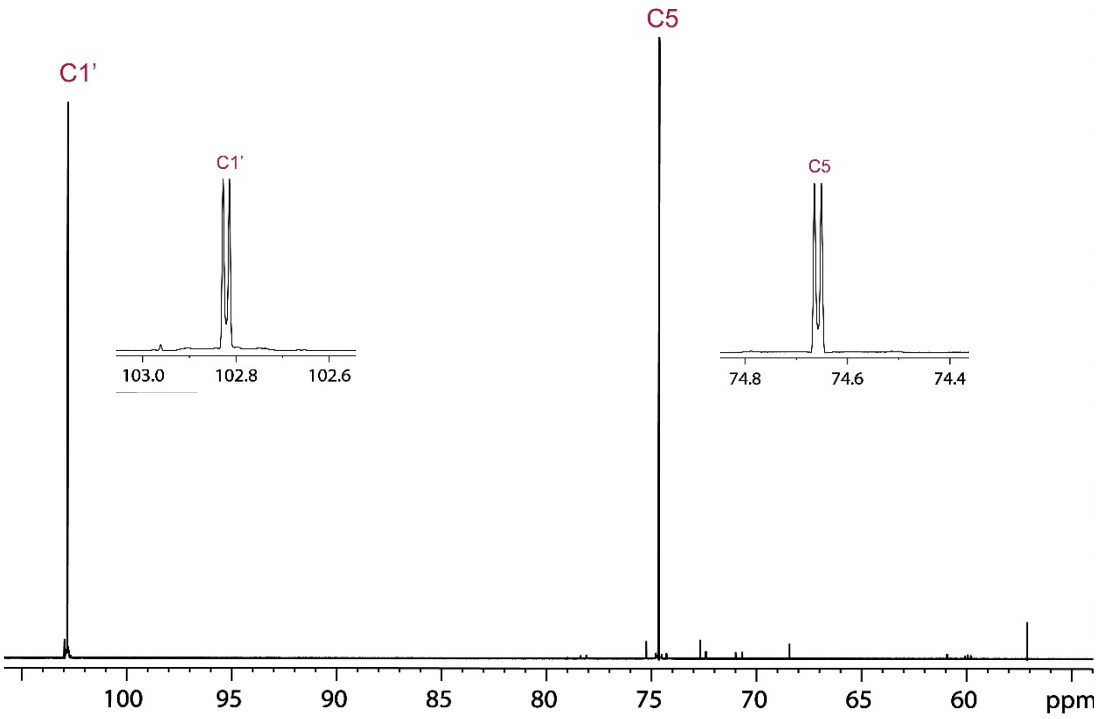

Figure S4. Partial $^{13}C\{^{1}H\}$ NMR spectrum (150 MHz) of methyl β-D-[1',5-$^{13}C_2$]lactoside (**2**$^{1',5}$). Signals labeled in red arise from the ^{13}C-labeled carbons, and the weak signals arise from the carbons at natural abundance. $^{3}J_{C1',C5}$ (2.0 Hz) was measured from the splitting of the C1' and C5 signals (insets).

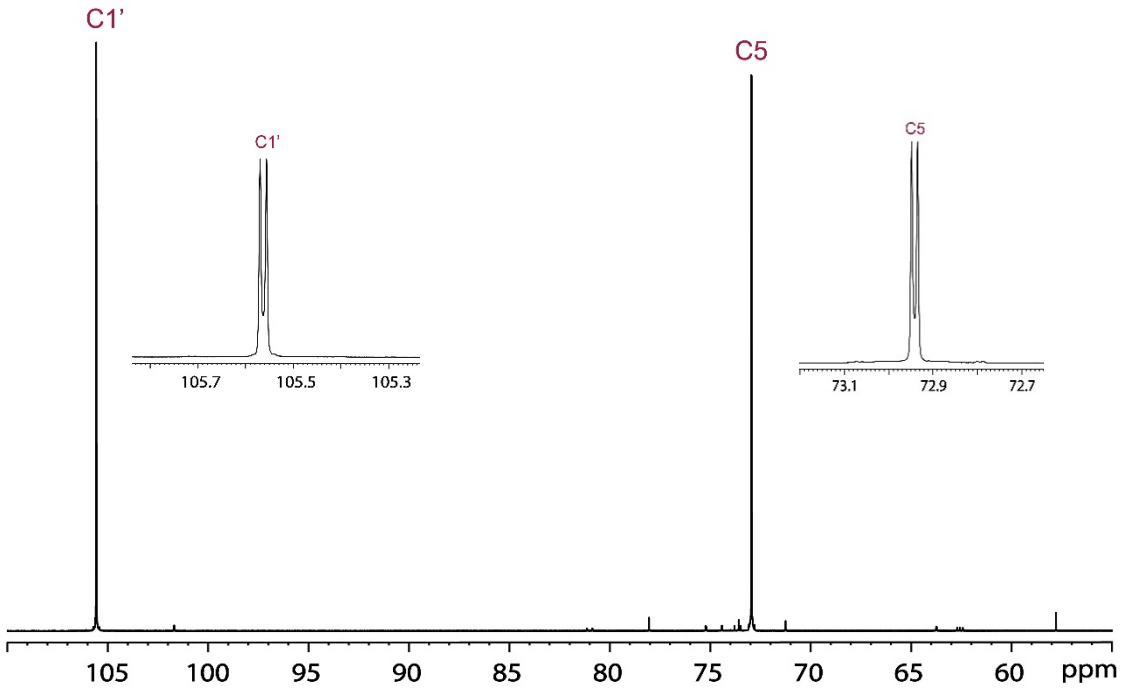

Figure S5. Partial $^{13}C\{^{1}H\}$ NMR spectrum (150 MHz) of methyl α-D-[1',5-$^{13}C_2$]lactoside (**4**$^{1',5}$). Signals labeled in red arise from the ^{13}C-labeled carbons, and the weak signals arise from the carbons at natural abundance. $^{3}J_{C1',C5}$ (2.0 Hz) was measured from the splitting of the C1' and C5 signals (insets).

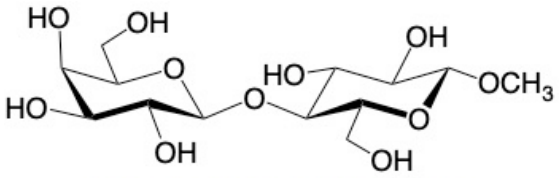

βGal-(1→4)-βGlcOCH$_3$ (**2**^{k})

C1'–C2'–O2'–H: Fixed 180°
C2'–C3'–O3'–H: Fixed 180°
C3'–C4'–O4'–H: Fixed 180°
C4'–C5'–C6'–O6: Fixed 180°
C5'–C6'–O6'–H: Fixed 180°
C4–C3–O3–H: Fixed 180°
C3–C2–O2–H: Fixed 180°
C4–C5–C6–O6: Fixed 180°
C5–C6–O6–H: Fixed 180°
C2–C1–O1–CH$_3$: Initial 180°

phi (ϕ) (O5'–C1'–O1'–C4): 15° rotations
psi (ψ) (C1'–O1'–C4–C3): 15° rotations

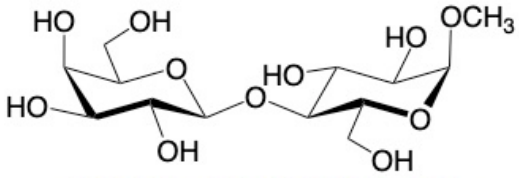

βGal-(1→4)-αGlcOCH$_3$ (**4**^{k})

C1'–C2'–O2'–H: Fixed 180°
C2'–C3'–O3'–H: Fixed 180°
C3'–C4'–O4'–H: Fixed 180°
C4'–C5'–C6'–O6: Fixed 180°
C5'–C6'–O6'–H: Fixed 180°
C4–C3–O3–H: Fixed 180°
C3–C2–O2–H: Fixed 180°
C4–C5–C6–O6: Fixed 180°
C5–C6–O6–H: Fixed 180°
C2–C1–O1–CH$_3$: Initial 180°

phi (ϕ) (O5'–C1'–O1'–C4): 15° rotations
psi (ψ) (C1'–O1'–C4–C3): 15° rotations

Scheme S2. Torsional constraints applied to **2**^{k} and **4**^{k} during DFT calculations of J_{CC} values.

Table S2. ^{1}H-^{1}H Spin-Couplings[a] in Methyl β-D-Glucopyranoside (**3**).

coupled nuclei	H1–H2	H2–H3	H3–H4	H4–H5	H5–H6	H5–H6’	H6–H6’
J_{HH}	8.0	9.4	9.1	9.9	2.3	6.1	(–) 12.4

[a]In Hz ± 0.1 Hz, in $^{2}H_2O$, 22 °C. H6’ is defined as the more shielded H6 hydrogen. The sign of the $^{2}J_{HH}$ value is assumed to be negative.

Table S3. Fitting Statistics[a] from Solid-State ^{13}C NMR Determinations of J_{CC} Values in Crystalline **2**$^{1',5}$, **3**^{1,2}, **3**^{1,3}, **3**^{1,6} and **4**$^{1',5}$.

cmpd	$^{n}J_{CC}$	detected spin	*J*-coupling (Hz)	standard error (Hz)	adjusted R^2	reduced chi^{2b}
3^{1,2}	$^{1}J_{C1.C2}$	C1	49.38	0.276	0.982	7.98
			48.76	0.220	0.988	5.19
			48.95	0.230	0.987	5.66
		C2	49.05	0.233	0.987	5.81
			49.19	0.245	0.986	6.43
			49.22	0.252	0.985	6.88
3^{1,3}	$^{2}J_{C1.C3}$	C1	5.20	0.035	0.996	0.506
			5.22	0.032	0.997	0.442
			5.21	0.036	0.996	0.536
		C3	5.20	0.044	0.994	0.848
			5.21	0.042	0.995	0.747
			5.21	0.047	0.994	0.935
3^{1,6}	$^{3}J_{C1.C6}$	C1	3.87	0.031	1.000	0.215
			3.87	0.034	0.994	0.265
			3.87	0.041	0.992	0.382
		C6	3.93	0.033	0.995	0.261
			3.98	0.031	1.000	0.239
			3.93	0.041	0.992	0.406
2$^{1',5}$	$^{3}J_{C1'.C5}$	C1'	4.66	0.047	0.992	0.731
			4.80	0.048	0.992	0.795
			4.69	0.055	0.990	1.01
		C5	4.81	0.077	0.981	2.10
			4.87	0.060	0.988	1.34
			4.79	0.080	0.979	2.24
4$^{1',5}$	$^{3}J_{C1'.C5}$	C1'	4.08	0.055	0.987	0.760
			4.06	0.049	0.989	0.603
			3.99	0.038	0.993	0.345
		C5	4.03	0.043	0.992	0.454
			4.04	0.056	0.986	0.772
			4.04	0.052	0.988	0.659

[a]Data were obtained from three experiments to measure the J_{CC} value in each compound. [b]Value x 10^4.

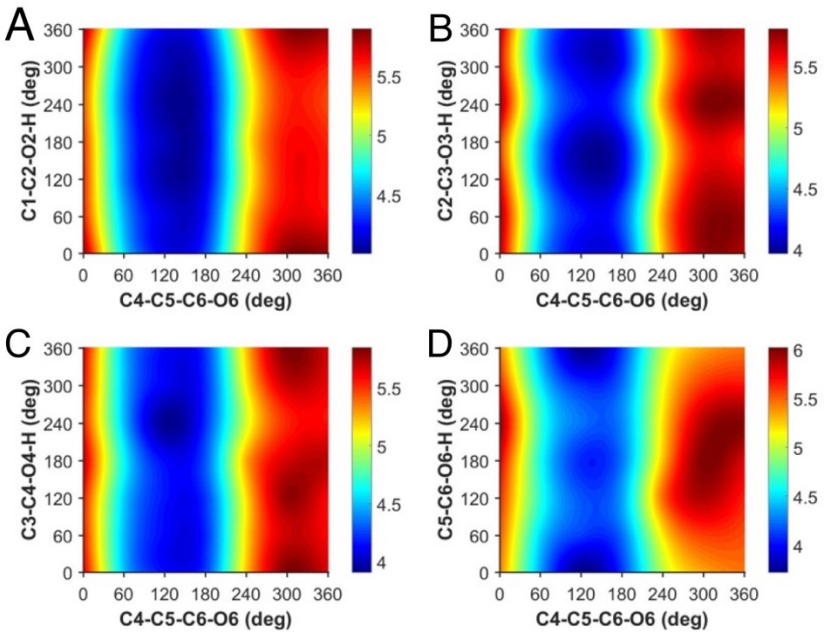

Figure S6. Contour plots of calculated $^{3}J_{C1,C6}$ values in **3**^{k} showing a primary on dependence the C4–C5–C6–O6 torsion angle and the effects on this dependency of rotating the C2–O2 (A), C3–O3 (B), C4–O4 (C) and C6–O6 (D) bonds in the structure.

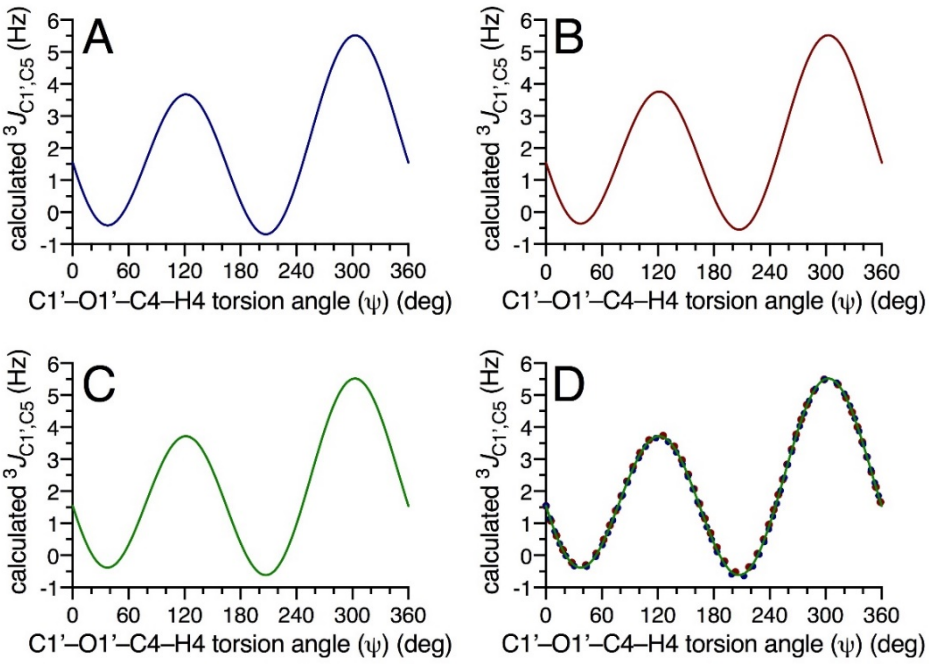

Figure S7. Plots of calculated $^3J_{C1',C5}$ values in **2**^{k} (A) and **4**^{k} (B) as a function of ψ. (C) Plot of average calculated $^3J_{C1',C5}$ values in **2**^{k} and **4**^{k}. (D) Superimposition of the plots in (A), (B) and (C); **2**^{k} (blue circles), **4**^{k} (red circles), averaged equation (green line).

Cartesian coordinates for DFT-optimized conformers of **2**^{k} – **4**^{k}
(ϕ and ψ are defined as O5'–C1'–O1'–C4 and C1'–O1'–C4–C3, respectively;

Structure **2**^{k}: ϕ = 0°, ψ = 0°.

C	3.587	1.201	0.375
C	2.156	1.589	0.002
C	3.014	-1.145	-0.194
C	3.644	-0.241	0.894
H	1.536	1.574	0.908
H	4.206	1.253	-0.534
H	3.609	-1.045	-1.117
H	4.697	-0.538	1.031
O	1.668	-0.734	-0.450
O	2.134	2.872	-0.612
H	2.514	3.483	0.041
O	4.022	2.173	1.321
H	4.932	1.959	1.583
O	2.946	-0.282	2.133
H	2.973	-1.188	2.475
C	2.989	-2.614	0.207
H	4.024	-2.928	0.409
H	2.412	-2.728	1.137
O	2.401	-3.379	-0.835
H	2.402	-4.305	-0.545
C	-1.059	-1.132	-0.587
C	-1.876	1.248	-0.276
C	-2.498	-1.545	-0.252
H	-1.387	1.343	0.707
C	-3.197	-0.499	0.604
H	-3.069	-1.628	-1.189
H	-2.679	-0.367	1.572
O	-3.196	0.732	-0.106
O	-4.509	-0.918	0.803
O	-2.411	-2.807	0.403
H	-3.321	-3.070	0.616
C	-5.222	-0.165	1.788
H	-4.710	-0.209	2.759
H	-5.328	0.882	1.483
H	-6.209	-0.623	1.876
C	-2.002	2.630	-0.902
H	-0.995	3.041	-1.039
H	-2.473	2.529	-1.892
O	-2.795	3.445	-0.042
H	-2.862	4.318	-0.460

C	-1.022	0.292	-1.154
H	-1.455	0.250	-2.162
C	1.565	0.567	-0.982
H	2.132	0.613	-1.930
O	0.246	0.953	-1.281
O	-0.553	-2.013	-1.583
H	-0.587	-2.906	-1.202
H	-0.461	-1.183	0.329

Structure **4**^{k}: $\phi = 0°$, $\psi = 0°$.

C	-1.379	-0.592	-1.093
C	-1.865	-1.675	-0.115
C	-3.320	-1.421	0.282
C	-3.503	-0.002	0.833
C	-2.943	0.977	-0.227
C	-3.017	2.432	0.217
C	3.338	0.761	0.520
C	2.537	1.779	-0.296
C	1.123	1.277	-0.623
C	1.181	-0.114	-1.258
C	2.100	-1.049	-0.428
C	2.340	-2.379	-1.127
O	-1.572	0.671	-0.496
O	-1.740	-2.946	-0.741
O	-3.656	-2.448	1.209
O	-2.821	0.068	2.080
O	-2.487	3.263	-0.805
O	-0.036	-0.862	-1.413
O	3.387	-0.453	-0.212
O	2.759	0.624	1.789
O	2.357	3.031	0.357
O	0.548	2.165	-1.577
O	3.188	-3.178	-0.306
H	-1.955	-0.649	-2.033
H	-1.234	-1.611	0.782
H	-3.943	-1.510	-0.623
H	-4.578	0.202	0.968
H	-3.533	0.864	-1.151
H	-4.069	2.669	0.433
H	-2.441	2.557	1.147
H	4.391	1.066	0.613
H	3.078	1.912	-1.244
H	0.538	1.248	0.300

H	1.602	0.007	-2.265
H	1.369	-2.859	-1.296
H	2.808	-2.187	-2.106
H	3.009	-0.162	3.644
H	3.604	-1.214	2.327
H	4.539	0.231	2.807
H	-2.057	-3.593	-0.089
H	-4.578	-2.321	1.487
H	-2.927	0.962	2.442
H	-2.550	4.179	-0.491
H	3.230	3.388	0.584
H	0.521	3.039	-1.154
H	3.326	-4.017	-0.771
H	1.616	-1.232	0.540
C	3.527	-0.180	2.683

Structure **3**^{k}:
[C2–C1–O1–CH_3 = C1–C2–O2–H = C2–C3–O3–H = C3–C4–O4–H = C4–C5–C6–O6 = C5–C6–O6–H = 180^{o}]

C	1.117	-0.668	0.181
C	1.246	0.724	-0.437
C	0.084	1.601	0.025
C	-1.272	0.936	-0.204
C	-1.256	-0.464	0.445
C	-2.526	-1.259	0.183
O	-0.171	-1.202	-0.124
O	2.079	-1.501	-0.372
O	2.489	1.291	-0.048
O	0.193	2.836	-0.675
H	2.875	-3.368	-0.339
O	-2.227	1.828	0.372
O	-2.409	-2.525	0.820
H	0.193	1.772	1.108
H	-3.387	-0.697	0.575
H	1.192	0.604	-1.530
H	-2.658	-1.371	-0.904
H	-1.114	-0.361	1.533
H	-3.227	-3.014	0.641
H	1.234	-0.608	1.279
C	2.049	-2.835	0.137
H	2.524	2.169	-0.463
H	-0.548	3.388	-0.376
H	-1.446	0.824	-1.285
H	1.104	-3.333	-0.102

H	2.194	-2.841	1.227
H	-3.116	1.460	0.257

Complete reference 40:

M. J. Frisch, G. W. Trucks, H. B. Schlegel, G. E. Scuseria, M. A. Robb, J. R. Cheeseman, G. Scalmani, V. Barone, B. Mennucci, G. A. Petersson, H. Nakatsuji, M. Caricato, X. Li, H. P. Hratchian, A. F. Izmaylov, J. Bloino, G. Zheng, J. L. Sonnenberg, M. Hada, M. Ehara, K. Toyota, R. Fukuda, J. Hasegawa, M. Ishida, T. Nakajima, Y. Honda, O. Kitao, H. Nakai, T. Vreven, J. A. Montgomery, Jr., J. E. Peralta, F. Ogliaro, M. Bearpark, J. J. Heyd, E. Brothers, K. N. Kudin, V. N. Staroverov, R. Kobayashi, J. Normand, K. Raghavachari, A. Rendell, J. C. Burant, S. S. Iyengar, J. Tomasi, M. Cossi, N. Rega, J. M. Millam, M. Klene, J. E. Knox, J. B. Cross, V. Bakken, C. Adamo, J. Jaramillo, R. Gomperts, R. E. Stratmann, O. Yazyev, A. J. Austin, R. Cammi, C. Pomelli, J. W. Ochterski, R. L. Martin, K. Morokuma, V. G. Zakrzewski, G. A. Voth, P. Salvador, J. J. Dannenberg, S. Dapprich, A. D. Daniels, Ö. Farkas, J. B. Foresman, J. V. Ortiz, J. Cioslowski, and D. J. Fox *Gaussian*09, Revision E.01**,** Gaussian, Inc., Wallingford CT, 2009.